RESEARCH ARTICLE
Editor's Choice
ADVANCED MATERIALS
www.advmat.de

Bonding Optimization Strategies for Flexibly Preparing Multi-Component Piezoelectric Crystals

Yuan Bai, Gang Tang, Lei Xie, He Lian, Shihao Wang, Chaopeng Liu, Qiao Yu, Jianying Ji, Kailiang Ren, Xiaodan Cao, Cong Li, Lili Zhou, Yizhu Shan, Hongyu Meng, and Zhou Li**

Flexible films with optimal piezoelectric performance and water-triggered dissolution behavior are fabricated using the co-dissolution–evaporation method by mixing trimethylchloromethyl ammonium chloride (TMCM-Cl), $CdCl_2$, and polyethylene oxide (PEO, a water-soluble polymer). The resultant TMCM trichlorocadmium (TMCM-$CdCl_3$) crystal/PEO film exhibited the highest piezoelectric coefficient (d_{33}) compared to the films employing other polymers because PEO lacks electrophilic or nucleophilic side-chain groups and therefore exhibits relatively weaker and fewer bonding interactions with the crystal components. Furthermore, upon slightly increasing the amount of one precursor of TMCM-$CdCl_3$ during co-dissolution, this component gained an advantage in the competition against PEO for bonding with the other precursor. This in turn improved the co-crystallization yield of TMCM-$CdCl_3$ and further enhanced d_{33} to ≈71 pC/N, exceeding that of polyvinylidene fluoride (a commercial flexible piezoelectric) and most other molecular ferroelectric crystal-based flexible films. This study presents an important innovation and progress in the methodology and theory for maintaining a high piezoelectric performance during the preparation of flexible multi-component piezoelectric crystal films.

1. Introduction

Transient electronic devices can be easily destroyed or degraded under environmental stimuli (e.g., water, heat, and light),[1] holding significant potential applications in biomedicine,[2] information security,[3] and degradable consumer electronics.[4] Flexible transient piezoelectric devices based on degradable flexible piezoelectric materials offer extensive application prospects in self-powered sensing, therapy, and energy harvesting devices.[5–7] Their performance and application critically depend on their flexibility, piezoelectric performance, and degradation behavior. Piezoelectric materials, as the core of these devices, are primarily classified into either rigid ceramics and crystals, or flexible piezoelectric polymers.[8,9] Although some ceramics exhibit high piezoelectric coefficients, they are prepared using energy- and time-consuming methods and do not degrade easily.[8] On the other hand, piezoelectric polymers are flexible, but their piezoelectric coefficients remain low, especially for polymers with transient responsiveness such as water solubility or degradability.[10,11] In recent years, some organic-inorganic two-component molecular ferroelectric crystals have demonstrated notable piezoelectric coefficients.[12–14] For instance, the longitudinal piezoelectric strain coefficients (d_{33}) of TMCM-$MnCl_3$ and TMCM-$CdCl_3$ (TMCM = trimethylchloromethyl ammonium) are 185 and 220 pC/N, respectively, reaching the level of commercial ceramic barium titanate (d_{33} = 203 pC/N).[15] These molecular ferroelectric crystals offer additional advantages such as straightforward fabrication and water solubility.[16–18] Combining the water-soluble multi-component molecular ferroelectric crystals with water-soluble polymers using the

Y. Bai, Q. Yu, J. Ji, K. Ren, X. Cao, C. Li, Y. Shan, H. Meng, Z. Li
Beijing Institute of Nanoenergy and Nanosystems
Chinese Academy of Sciences
Beijing 101400, China
E-mail: menghy@iccas.ac.cn; zli@binn.cas.cn

Y. Bai, Q. Yu, J. Ji, K. Ren, X. Cao, C. Li, Z. Li
Center on Nanoenergy Research
School of Physical Science and Technology
Guangxi University
Nanning 530004, China

G. Tang, S. Wang
Advanced Research Institute of Multidisciplinary Science
Beijing Institute of Technology
Beijing 100081, China

L. Xie, C. Liu
School of Minerals Processing and Bioengineering
Central South University
Changsha 410083, China

H. Lian, Z. Li
Department of Biomedical Engineering
School of Medical Instrumentation
Shenyang Pharmaceutical University
Shenyang 110016, China

K. Ren, L. Zhou, Y. Shan, H. Meng, Z. Li
School of Nanoscience and Technology
University of Chinese Academy of Sciences
Beijing 100049, China

The ORCID identification number(s) for the author(s) of this article can be found under https://doi.org/10.1002/adma.202411589

DOI: 10.1002/adma.202411589

co-dissolution–evaporation method can fabricate high piezoelectric flexible materials with water-triggered dissolution behavior straightforwardly.

In a previous study, a flexible TMCM-$CdCl_3$/polydimethylsiloxane (PDMS) piezoelectric film demonstrating remarkable d_{33}, and output power density was prepared by mixing TMCM-$CdCl_3$ powders of a uniform (micrometer) size with PDMS precursor in a complicated manner.[19] However, there is little research on fabricating multi-component crystals-based flexible transient piezoelectric films using co-dissolution-evaporation method,[20,21] and there are no known strategies or related mechanisms for improving the piezoelectric performance. We believe that the co-crystallization yield of multi-component crystal after co-dissolution-evaporation is a key factor affecting the piezoelectric performance of the multi-component crystal/polymer composite film.[22–24] This aspect deserves a detailed investigation.

In this study, we attempted to improve the co-crystallization yield of TMCM-$CdCl_3$ using two strategies. 1) We optimized the water-soluble polymers and found that the electrophilic or nucleophilic side-chain groups of different polymers tended to form more numerous and stronger bonding interactions (such as ionic, hydrogen, halogen, coordination, and other bonds).[25–29] with the groups or ions from the two components of TMCM-$CdCl_3$ (TMCM$^+$ and $[CdCl_3]^-$) in the solution. Such enhanced bonding has a significant inhibitory effect on the crystallization of TMCM-$CdCl_3$ in the composite film. In comparison, polyethylene oxide (PEO), which does not contain electrophilic or nucleophilic side-chain groups, has a relatively smaller negative impact on crystallization.[30] As a result, the composite film prepared from PEO and TMCM-$CdCl_3$ (or its two precursors, namely TMCM-Cl and $CdCl_2$) displayed the highest d_{33} values. 2) We also optimized the molar ratio between the two precursors of TMCM-$CdCl_3$. By slightly increasing the amount of either component during co-dissolution, this component gains an advantage in the competition against PEO for bonding with the other component. Such a change enhances the crystallization yield of TMCM-$CdCl_3$ in the composite film and further improves the d_{33} value to ≈71 pC/N, exceeding that of polyvinylidene fluoride (PVDF, a commercial flexible piezoelectric) and most other molecular ferroelectric crystal-based flexible films reported previously. This study highlights the influences of soluble polymers with different groups and ratios between crystal components on the piezoelectric performance of composite films, as well as the underlying mechanism. Our additional experiments also demonstrated that piezoelectric sensors based on the TMCM-$CdCl_3$/PEO film were sufficiently sensitive to recognize diverse movements of human fingers, and the TMCM-$CdCl_3$/PEO film could be dissolved rapidly in water, and then recycled with feasible approach.

2. Results and Discussion

2.1. Performance of Different TMCM-$CdCl_3$/Polymer Films

To prepare high piezoelectric TMCM-$CdCl_3$/polymer films with water-triggered degradation behavior through co-dissolution–evaporation, and to investigate the various effects of polymer possessing different groups on co-crystallization and piezoelectric performance, a total of six different water-soluble polymers with linear structures were tested: PEO, polyvinyl alcohol (PVA), polyacrylamide (PAM), gelatin, pullulan, and poly(acrylic acid) (PAA) (**Figure 1a,b**).[31] The six polymers exhibit distinct structural attributes (Figure 1a): PEO consists of [-CH_2-CH_2-O-] repeating units and no side-chain groups. PVA has an alkane main chain consisting of [-CH_2-CH(OH)-] repeating units and numerous hydroxyl (-OH) side groups. PAM has an alkane main chain consisting of [-CH_2-CH($CONH_2$)-] repeating units, and each repeating unit carries an amide (-$CONH_2$) side group. Gelatin is a protein consisting of glycine-proline-X (X = another amino acid) and glycine-X-hydroxyproline segments in a specific ratio, along with some amino acid-derived side-chain groups including amine, carboxyl, amide, hydroxyl, and other groups. As a polysaccharide, pullulan comprises repeating maltotriose units, with glycosidic bonds (ether bonds) linking the sugar units in the main chain and abundant hydroxyl groups as its side groups. PAA has an alkane main chain structure consisting of [-CH_2-CH(COOH)-] repeating units, and each unit contains a carboxylic acid (-COOH) side group.

In TMCM-Cl, one of the two precursors of TMCM-$CdCl_3$, ionic bonds are formed between Cl^- and TMCM$^+$. In the other precursor ($CdCl_2$), the two Cl^- form ionic bonds with Cd^{2+}. After dissolving both precursors in water, the ions undergo re-coordination to form TMCM$^+$ and $[CdCl_3]^-$. When their molar ratio is 1:1, TMCM$^+$ and $[CdCl_3]^-$ are connected through C—Cl···Cl—Cd interactions, and the inorganic anion layer of $[CdCl_3]^-$ and organic cation layer of TMCM$^+$ are alternately stacked. Upon the complete evaporation of water, TMCM-$CdCl_3$ molecular ferroelectric crystals with high piezoelectric properties are formed.[15,32] When a water-soluble polymer is present during the crystallization, chemical groups of the polymer can form ionic, hydrogen, or halogen bonds with the ions or atoms in $[CdCl_3]^-$ or TMCM$^+$, exerting various inhibitory effects on the crystallization or recrystallization yield of TMCM-$CdCl_3$ in the composite films. A greater inhibitory effect is expected to lead to a lower d_{33} value of the TMCM-$CdCl_3$/polymer film.

According to our experimental results, TMCM-$CdCl_3$/PEO films exhibit the highest average d_{33} compared with other composite films (Figures 1c and S1, Supporting Information), prepared with the mass ratio of TMCM-$CdCl_3$ to water-soluble polymer as 2:3. It is inferred that because PEO lacks electrophilic or nucleophilic side-chain groups, it mainly interacts with the components of TMCM-$CdCl_3$ by forming halogen bonds (C—Cl···O—C bonds) through its main-chain ether group,[33] as well as coordination bonds with Cd^{2+}.[34,35] Consequently, compared with the other polymers carrying various side groups, PEO forms fewer and weaker bonding interactions with -Cl, Cl^-, and Cd^{2+}, thus exerting a lesser inhibitory effect on the crystallization yield of TMCM-$CdCl_3$ and resulting in the highest d_{33} for the TMCM-$CdCl_3$/PEO film. In comparison, PAA, which contains numerous side-chain carboxylate and carboxylic acid groups when dissolved in water, had the most negative impact on TMCM-$CdCl_3$ crystallization. The carboxylate groups can form strong ionic bonds with both TMCM$^+$ and Cd^{2+},[25,36] and the carboxylic acid side groups of PAA also form C═O···Cl and H—O···Cl halogen bonds,[37,38] O—H···Cl hydrogen bonds,[39] and Cd^{2+}-based coordinate bonds with the TMCM-$CdCl_3$ components.[40] Thus, PAA strongly interferes with the halogen···halogen interactions (C—Cl···Cl—Cd) between the two components of

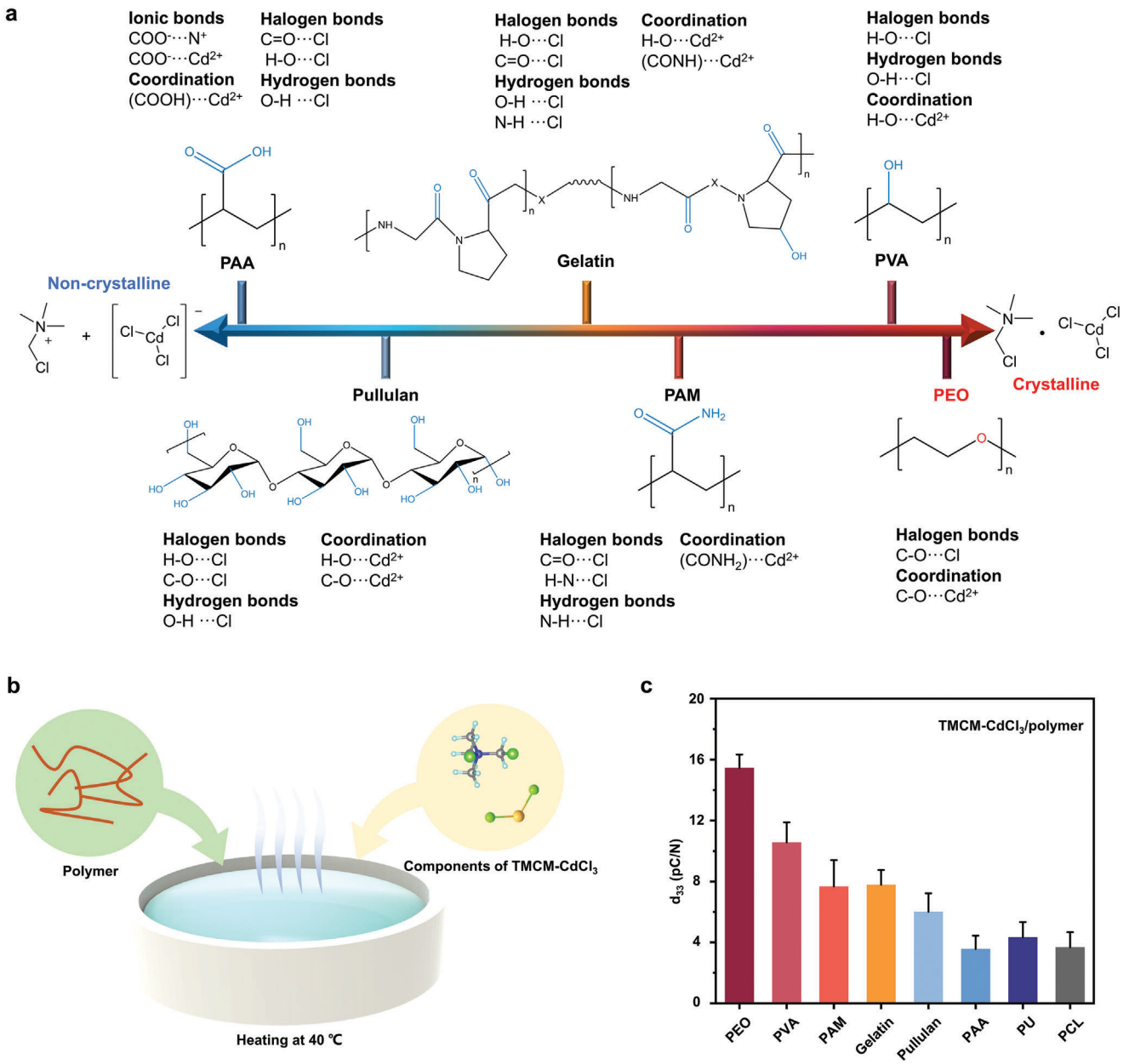

Figure 1. Preparation and characterization of TMCM-$CdCl_3$/polymer composite films. a) Schematic comparison of the inhibitory effects of six polymers on the crystallization of TMCM-$CdCl_3$ and the corresponding bonding interactions. b) Schematic of the co-dissolution–evaporation method. c) d_{33} values of different TMCM-$CdCl_3$/polymer composite films. (n = 10 independent spot d_{33} measurements on a film. Data are presented as mean ± standard deviation).

TMCM-$CdCl_3$,[32,41] thus reducing the binding efficiency of $TMCM^+$ and $[CdCl_3]^-$. All these effects severely inhibit the formation and growth of TMCM-$CdCl_3$ crystals in the composite film, reducing the crystallization yield and leading to the smallest d_{33} value of the TMCM-$CdCl_3$/PAA film (below 5 pC/N). Composite films based on the other four water-soluble polymers (PVA, gelatin, PAM, and pullulan) showed intermediate d_{33} values of 5–10 pC/N (Figure 1c). On the one hand, the side-chain groups of these four polymers (such as hydroxyl and amide groups) form various hydrogen, halogen, and/or coordination bonding interactions with chemical groups or ions in the TMCM-$CdCl_3$ components, though these interactions are still weaker than the ionic bonding interaction between the carboxylate groups of PAA and $TMCM^+$ or Cd^{2+}.[42] On the other hand, compared to PEO, all these four polymers exhibit denser interactions with the TMCM-$CdCl_3$ components. Specifically, the side-chain hydroxyl groups of PVA and pullulan form not only H—O···Cl halogen bonds[39] and Cd^{2+}-based coordinate bonds[28] similar to the case of PEO, but also O—H···Cl hydrogen bonds with Cl atoms and ions of $TMCM^+$ and $[CdCl_3]^-$.[39] Similarly, the side-chain amide groups in PAM tend to form C = O···Cl halogen bonds, H—N···Cl halogen bonds, coordination bonds, and N-H···Cl hydrogen bonds

with the two components.[37,43–45] The few residual carboxylate groups in PAM can also form ionic bonds with $TMCM^+$ and Cd^{2+}. The diverse chemical groups contained in gelatin are involved in different types of bonding interactions, including halogen, hydrogen, ionic, and coordination bonding, with the components of TMCM-$CdCl_3$.

Because the TMCM-$CdCl_3$ crystals and their two precursors are also soluble in the organic solvent dimethylformamide (DMF), we also prepared TMCM-$CdCl_3$/PU and TMCM-$CdCl_3$/PCL films in DMF (PCL = polycaprolactone, PU = polyurethane) using the DMF-soluble PU and PCL. However, their d_{33} values were lower compared to those of the composite films based on the most water-soluble polymers. We infer that the main-chain carbamate bonds or ester bonds of PU or PCL, together with DMF molecules, tend to form different interactions with the ions and groups of $TMCM^+$ and $[CdCl_3]^-$,[46] severely affecting the crystallization yield and resulting in a lower d_{33} of the TMCM-$CdCl_3$/PU and TMCM-$CdCl_3$/PCL films (Figure 1c). The d_{33} value of different TMCM-$CdCl_3$/polymer films generally showed a positive correlation with the intensity of the characteristic peaks of TMCM-$CdCl_3$ crystal in corresponding TMCM-$CdCl_3$/polymer film through X-ray diffraction (XRD) analysis (Figure S2, Supporting Information, Figure 1c). Meaningfully, during flexibly preparing other water-soluble piezoelectric crystals, such as tetramethylammonium tetrachloroferrate ($[(CH_3)_4N][FeCl_4]$),[47] PEO also exhibits sufficient advantages in terms of the piezoelectric coefficient (Figures S3, S4, Supporting Information).

To explain how the bonding interactions vary depending on the type of polymer, we conducted quantitative comparison of adhesion energies between different polymer and TMCM-$CdCl_3$ components using atomic force microscopy (Figure S5, Supporting Information),[48,49] and by Density functional theory (DFT) calculations of the integrated crystal orbital Hamilton population (ICOHP) values of halogen and hydrogen bonds formed between polymers and TMCM-$CdCl_3$.[50–53] The comparison results of adhesion energies (Figures S6–S8, Supporting Information), and calculated |ICOHP| values (Figure S9, Table S1, Supporting Information) are consistent with the comparison of bonding interactions described above. Furthermore, we demonstrated the existence of the bonding interaction between polymers and Cl element of TMCM-$CdCl_3$ by comparing the infrared spectra of TMCM-$CdCl_3$/polymer films and TMCM-$CdCl_3$ crystals (Figure S10, Supporting Information). We also found evidence of incomplete co-crystallization of TMCM-Cl and $CdCl_2$ from SEM images and energy dispersive spectroscopy (EDS) maps of TMCM-$CdCl_3$/polymer (Figures S11–S15, Supporting Information), which is the phenomenon caused by of the bonding interaction of the polymer on TMCM-$CdCl_3$ components.

2.2. Performance of TMCM-$CdCl_3$/PEO Films

Among the water-soluble TMCM-$CdCl_3$/polymer films, the one based on PEO exhibited the highest d_{33} value. This d_{33} could be further enhanced by adjusting the mass ratio of TMCM-$CdCl_3$ to PEO. Upon gradually increasing the mass ratio of TMCM-$CdCl_3$ (defined as the total mass of TMCM-Cl and $CdCl_2$) to PEO from 1:3 to 3:2, the average d_{33} steadily increased to reach ≈32 pC/N (**Figure 2a**), which is close to the value of commercial PVDF (≈27 pC/N). The $[(CH_3)_4N][FeCl_4]$/PEO composite films showed the same trend as the TMCM-$CdCl_3$/PEO composite films: as the mass ratio of $[(CH_3)_4N][FeCl_4]$:PEO increased, the maximum d_{33} reached 4.8 pC/N (Figure S16, Supporting Information). XRD analysis revealed that upon increasing the mass ratio of TMCM-$CdCl_3$:PEO in the solution, characteristic peaks of the TMCM-$CdCl_3$ crystals (corresponding to the (110), (020), (200), (130), and (220) planes) in the composite film became gradually more intense (Figures 2b and S17, Supporting Information). This indicates that a higher ratio of TMCM-$CdCl_3$ components in the solution resulted in more TMCM-$CdCl_3$ crystals, thereby increasing the d_{33} value of the composite film. Scanning electron microscopy (SEM) analysis of the top surface of TMCM-$CdCl_3$/PEO films revealed that the orderly arranged and rod-shaped TMCM-$CdCl_3$ crystals gradually became larger in size at higher mass ratios of the two TMCM-$CdCl_3$ components (Figure 2c). A sufficiently large crystal size also helps improve the piezoelectric properties.[54] However, upon further increasing the mass ratio of TMCM-$CdCl_3$:PEO to 2:1 during dissolution, the integrity and morphology of the composite film after drying were significantly impaired (Figure S18, Supporting Information). A likely reason is that the excess TMCM-$CdCl_3$ components bond with and disperse in PEO, thereby deteriorating the film-forming performance and mechanical properties of the film.

Our cross-sectional SEM and EDS analyses (Figure 2d) revealed a sandwich structure in the TMCM-$CdCl_3$/PEO composite film with three clearly defined layers. The middle layer (≈41.63 μm in thickness) primarily consisted of TMCM-$CdCl_3$ crystals and their components, because the Cd and Cl elements were mainly concentrated in this layer. The top and bottom layers (≈2.83 and ≈4.36 μm in thickness, respectively) contained abundant oxygen (O) atoms, which only existed in PEO, along with trace amounts of Cd, N, and Cl, which are characteristic of $CdCl_2$ and TMCM-Cl. The bonding between the PEO and TMCM-$CdCl_3$ components in solution prevented a portion of $CdCl_2$ and TMCM-Cl from forming TMCM-$CdCl_3$ crystals (i.e., it resulted in a lowered crystallization yield of TMCM-$CdCl_3$), leading to their dispersion in PEO instead. This is one reason why the d_{33} value of the composite film was still significantly smaller than that of pure TMCM-$CdCl_3$ crystal (≈32 vs ≈220 pC/N).

When TMCM-Cl and $CdCl_2$ are combined in a 1:1 molar ratio, they meet the stoichiometric requirement to form TMCM-$CdCl_3$ crystals, and the increase of only either TMCM-Cl or $CdCl_2$ precursor during crystal preparation cannot change the molar ratio of the two components in the TMCM-$CdCl_3$ crystal.[15] During preparing TMCM-$CdCl_3$/PEO film, the main-chain ether bonds of PEO can form C—Cl···O—C halogen bonds with the Cl atoms of $TMCM^+$,[33] and these halogen bonds interfere with the C—Cl···Cl—Cd interactions in TMCM—$CdCl_3$, affecting the formation and growth of TMCM-$CdCl_3$ crystals in the composite film. Surprisingly, when either TMCM-Cl or $CdCl_2$ is in slight excess compared to the other, this component gains an advantage in competing with PEO for bonding with the other precursor, which improves the crystallization yield of TMCM-$CdCl_3$ in the composite film and leads to a further improvement in d_{33} to reach ≈71 pC/N (Figure S19, Supporting Information). Based on the high piezoelectric TMCM-$CdCl_3$/PEO film (d_{33} = ≈32 pC/N) prepared at the mass ratio of TMCM-$CdCl_3$:PEO = 3:2, we increased the

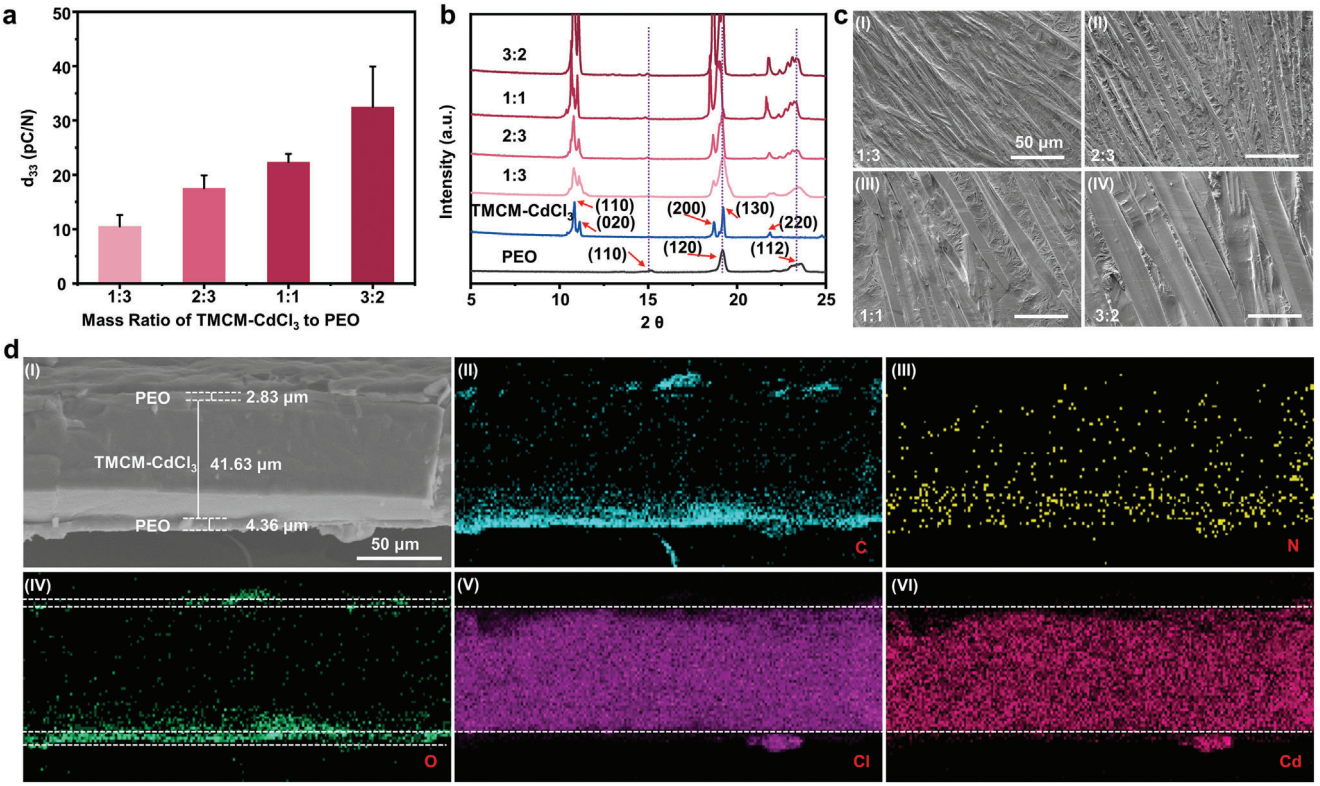

Figure 2. Characterization of TMCM-$CdCl_3$/PEO composite films. a) The d_{33} values (n = 10 independent spot d_{33} measurements on a film. Data are presented as mean ± standard deviation.), b) XRD patterns, and c) top-surface SEM images of films prepared at different TMCM-$CdCl_3$:PEO mass ratios. d) Cross-sectional SEM image and EDS maps of a sandwich-structured film prepared with a TMCM-$CdCl_3$:PEO mass ratio of 3:2.

amount of either TMCM-Cl or $CdCl_2$ within a certain range during co-dissolution; consequently, the d_{33} values were improved obviously. Specifically, when the molar ratio of TMCM-Cl: $CdCl_2$ was slightly changed from 1:1 to 1.2:1 or 1:1.2, the highest average d_{33} values were achieved, which were ≈60 or ≈44 pC/N, respectively. However, upon further increasing the molar ratio to 1.5:1, 1.7:1, and 2:1 by adding the amount of TMCM-Cl, d_{33} decreased to 46, 33, and 31 pC/N, respectively. A similar trend was observed when this ratio was further reduced to 1:1.5, 1:1.7, and 1:2 by increasing the amount of $CdCl_2$, with progressively lower d_{33} values of 34, 27, and 25 pC/N, respectively (**Figure 3b**). The d_{33} values of different TMCM-$CdCl_3$/PEO films generally showed a positive correlation with the intensity of the characteristic peaks of TMCM-$CdCl_3$ crystal in corresponding TMCM-$CdCl_3$/PEO film through XRD analysis (Figure S20, Supporting Information; Figure 3b). The excess amount of one component (either TMCM-Cl or $CdCl_2$) enhanced the crystallization yield of the other component, while the further excess component tended to disperse in the PEO matrix or among TMCM-$CdCl_3$ crystals, inhibiting the growth and arrangement of the TMCM-$CdCl_3$ crystals. Therefore, the piezoelectric performance prepared with further excess of one component was poorer than for the cases when one component was only in slight excess. Notably, further excess TMCM-Cl is more likely to damage the morphology of the composite film (Figure S21, Supporting Information), because as an organic molecule, it more readily disperses in the PEO matrix and bonds with PEO, thereby deteriorating the mechanical properties and film-forming performance. In brief, by interfering in the bonding interaction with PEO, slightly increasing the amount of one component can improve the coordination and co-crystallization yield of the two components in the composite film and enhance the d_{33} value (≈71 pC/N) of the TMCM-$CdCl_3$/PEO film to exceed that of the commercial piezoelectric PVDF and most other previously reported flexible films based on molecular ferroelectric crystals (Figure 3a,c).[19,20,22,55–67] This phenomenon and its mechanism also apply to the $[(CH_3)_4N][FeCl_4]$/PEO composite film (Figure S22, Supporting Information).

Although TMCM-$CdCl_3$ crystals are important for piezoelectric performance, their inherent rigidity poses a challenge for flexible systems, whereas the pliable PEO enhances the flexibility and mechanical stability of the composite films. The stress–strain curves of composite films with different component ratios indicated favorable tensile properties up to a strain of 0.2% (**Figure 4a**). The elastic moduli of all four TMCM-$CdCl_3$/PEO composite films were below 1 GPa (Figure 4b), with a maximum value of 0.81 GPa (for the film prepared with a TMCM-$CdCl_3$:PEO mass ratio of 1:3) and a minimum value of 0.28 GPa (for the film prepared with a TMCM-$CdCl_3$:PEO mass ratio of 3:2 and a TMCM-Cl:$CdCl_2$ molar ratio of 1.2:1), indicating their excellent flexibility. Interestingly, the elastic modulus also showed a decreasing trend as the increase of the size of rod-shaped TMCM-$CdCl_3$ crystals (Figure 2c), because larger crystals embedded in the PEO matrix tend to disrupt the compactness of the film more severely, leading to a further decrease in modulus. We also

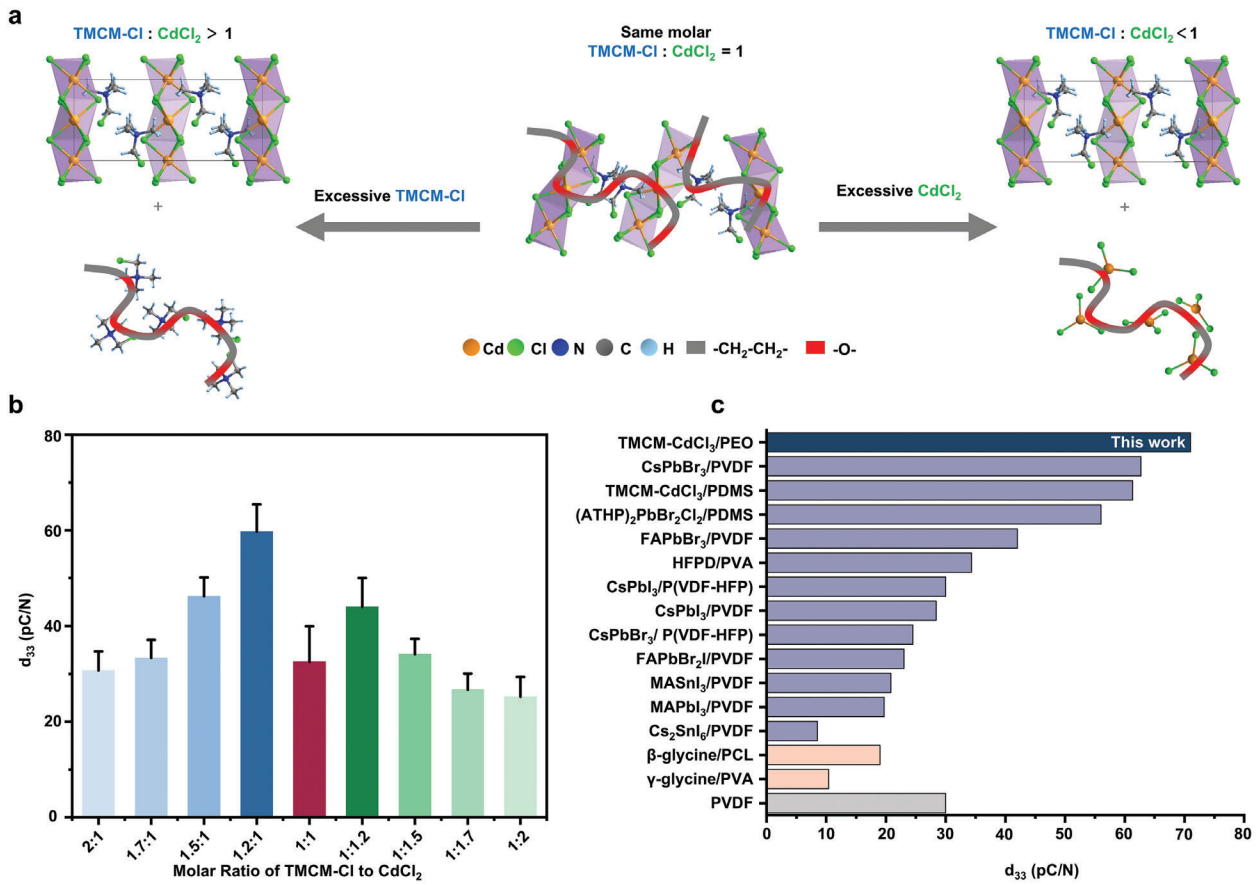

Figure 3. Competition mechanism in the TMCM-$CdCl_3$/PEO composite films. a) Schematic depicting improvement in the crystallization yield of TMCM-$CdCl_3$ by slightly increasing the amount of one crystal component to compete against PEO for bonding with the other component. b) d_{33} values of TMCM-$CdCl_3$/PEO films with one crystal component in excess: the molar ratio of TMCM-Cl:$CdCl_2$ ranged from 2:1 to 1:2. (n = 10 independent spot d_{33} measurements on a film. Data are presented as mean ± standard deviation.) c) Comparison of d_{33} values in this work with those of other previously reported molecular ferroelectric crystal-based flexible composite films.[19,20,22,56–68]

investigated the dynamic mechanical response of the films at various strain frequencies and amplitudes. When the strain was constant at 0.1% while the frequency was increased from 0.1 to 80 Hz, the elastic modulus of the composite films only showed a slight and gradual increase (Figure 4c). When the strain frequency was fixed at 1 Hz while the strain amplitude increased from 0.005% to 0.2%, the elastic modulus showed a slight and gradual decrease (Figure 4d). Fracture response was not observed in any film. Notably, the TMCM-$CdCl_3$/PEO film with slight excess TMCM-Cl (molar ratio of TMCM-Cl:$CdCl_2$ = 1.2:1) achieved a lower elastic modulus and better flexibility (Figure 4b) as well as better mechanical stability (Figure 4c,d) owing to the excess TMCM-Cl.

2.3. Piezoelectric Sensors Based on TMCM-$CdCl_3$/PEO Piezoelectric Films

We constructed flexible piezoelectric sensors based on the TMCM-$CdCl_3$/PEO piezoelectric composite films (**Figure 5a**). The fabrication process is detailed in Section 4 "Experimental Section." The flexible piezoelectric sensors consisted of three main components: a TMCM-$CdCl_3$/PEO piezoelectric film, iron electrodes, and polylactic acid (PLA) encapsulation layers. All the components were tightly interconnected and exhibited excellent flexibility. The operating principle of these sensors is illustrated in Figure 5b.[69] Initially, the dipoles in the TMCM-$CdCl_3$/PEO film are in equilibrium. Under externally applied pressure, the electric dipoles become polarized, causing an asymmetric distribution of positive and negative charges at the two surfaces of the film. Electrons induced on the electrodes flow through the external circuit to produce an electric current. When the pressure is removed, the device recovers from deformation and generates the opposite current. The output of the piezoelectric sensors was measured (Figure 5c–e). The open-circuit voltage, short-circuit current, and transferred charge all increased with increasing the TMCM-$CdCl_3$:PEO mass ratio, with maximum values of ≈5.9 V, 139.8 nA, and 3.0 nC, respectively, achieved from the film prepared with a TMCM-$CdCl_3$:PEO mass ratio of 3:2 and a TMCM-Cl:$CdCl_2$ molar ratio of 1.2:1.

We also investigated the sensor output at frequencies ranging from 1 to 3 Hz (Figure 5f). This frequency range matches the requirements for the sensing and energy harvesting of human motion.[70] The results showed an increase in the voltage from

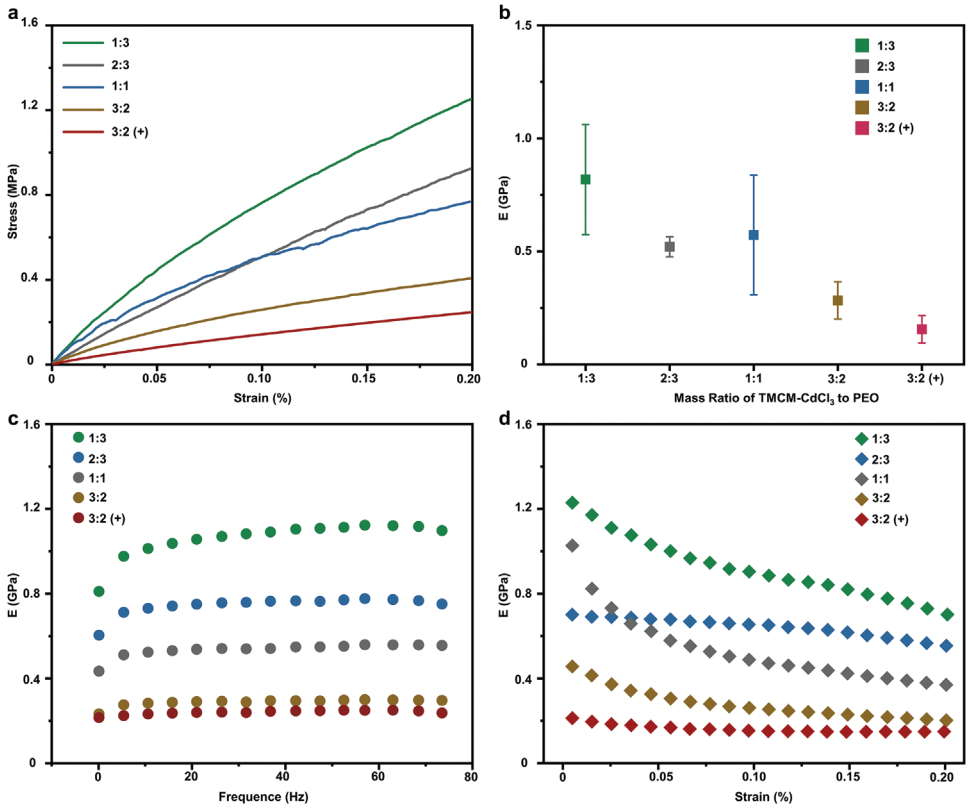

Figure 4. Mechanical performance of TMCM-$CdCl_3$/PEO films. a) Stress–strain curves. b) Elastic moduli calculated from the stress–strain curves in a). c) Dynamic mechanical analysis in the frequency sweep mode from 0.1 to 80 Hz at a constant strain of 0.1%. d) Dynamic mechanical analysis in the strain sweep mode from 0.005% to 0.2% strain at a constant frequency of 1 Hz. The films were prepared with mass ratios of TMCM-$CdCl_3$:PEO ranging from 1:3 to 3:2. The TMCM-$CdCl_3$/PEO film (denoted as "3:2 (+)") was prepared with a TMCM-$CdCl_3$:PEO mass ratio of 3:2 and a TMCM-Cl:$CdCl_2$ molar ratio of 1.2:1.

5.7 to 10.4 V with increasing frequency. Long-term operational stability is crucial for the application of wearable sensors. The device exhibited excellent stability, maintaining over 90% of its output performance even after continuous operation for 10 000 s. We performed two experiments for sensing the motions of the human hand (Figure 5h). In the first experiment, a piezoelectric sensor was attached to the index finger joint (Figure 5i). Bending the finger at 30, 60, and 90° generated signal outputs of 0.3, 0.6, and 0.8 V, respectively. In the second experiment, an array of five small sensors was placed on the back of the hand (Figure 5j). When one of the fingers taps on a table, the sensor closest to this finger is expected to produce a stronger signal. Different signal combinations are generated when the volunteer taps different fingers, allowing distinction of the specific finger. In summary, the developed piezoelectric sensor is capable of not only detecting the bending angle of a single finger when placed directly over the joint but also capturing complex finger movements when deployed as a sensor array on the back of the hand.

2.4. Dissolution and Recycling of Film Components

Because both PEO and TMCM-$CdCl_3$ crystals are water-soluble, their composite film dissolves almost instantaneously in water. When a piece of the TMCM-$CdCl_3$/PEO composite film (1 cm × 1 cm) was soaked in water under gentle stirring, it shrank rapidly, broke into small pieces, and then dissolved within seconds (**Figure 6a**). Thus, this film has good application potential in water-triggered flexible transient electronics. However, the toxic Cd from TMCM-$CdCl_3$ should be removed and recovered to avoid pollution risks. Therefore, we developed a recycling strategy for the film based on separation and dialysis (Figure 6b). After dissolving the composite film, the PLA encapsulation layers and Fe electrode could be easily separated, which can be further recycled or processed as biodegradable materials. The mixed solution was then subjected to dialysis to separate the TMCM-$CdCl_3$ components from PEO. TMCM-$CdCl_3$ crystals could be regenerated by evaporating the dialysate with a recovery rate of up to 97.96% (Figures 6b and S23, Supporting Information). The regenerated TMCM-$CdCl_3$ powder exhibited XRD peaks similar to those of the pure TMCM-$CdCl_3$ crystal, without the (110) and (112) diffraction peaks associated with PEO, demonstrating the successful separation and recycling of TMCM-$CdCl_3$ crystals (Figure 6c). Meanwhile, PEO could be precipitated and recycled by evaporating the solution remaining in the dialysis bag. Thus, we successfully separated and recycled most components of the piezoelectric sensor.

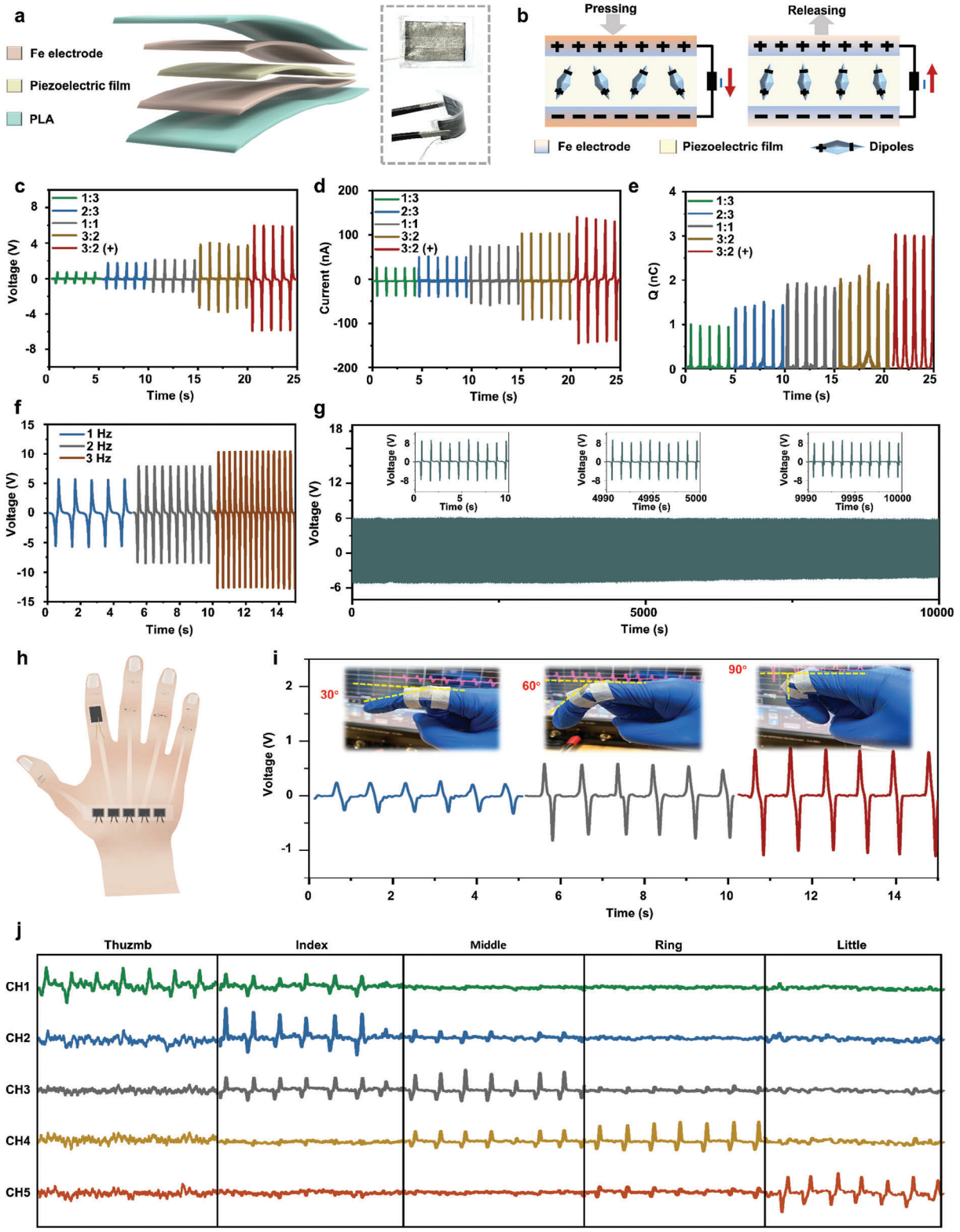

Figure 5. Performance of the flexible piezoelectric sensor based on TMCM-$CdCl_3$/PEO films. a) Schematic diagram and photographs of the sensor. b) Working principle of the sensor. c–e) Electric outputs of the sensors: c) voltage, d) current, and (e) charge under a pulsed 5 N force. f) Variation in the voltage with frequency. g) Durability test. h) Schematic of the sensor placements on the hand. i) Signals from the sensor attached to the index finger joint when bending the finger at different angles. j) Signals from an array of sensors placed on the back of the hand when different fingers tap on the table.

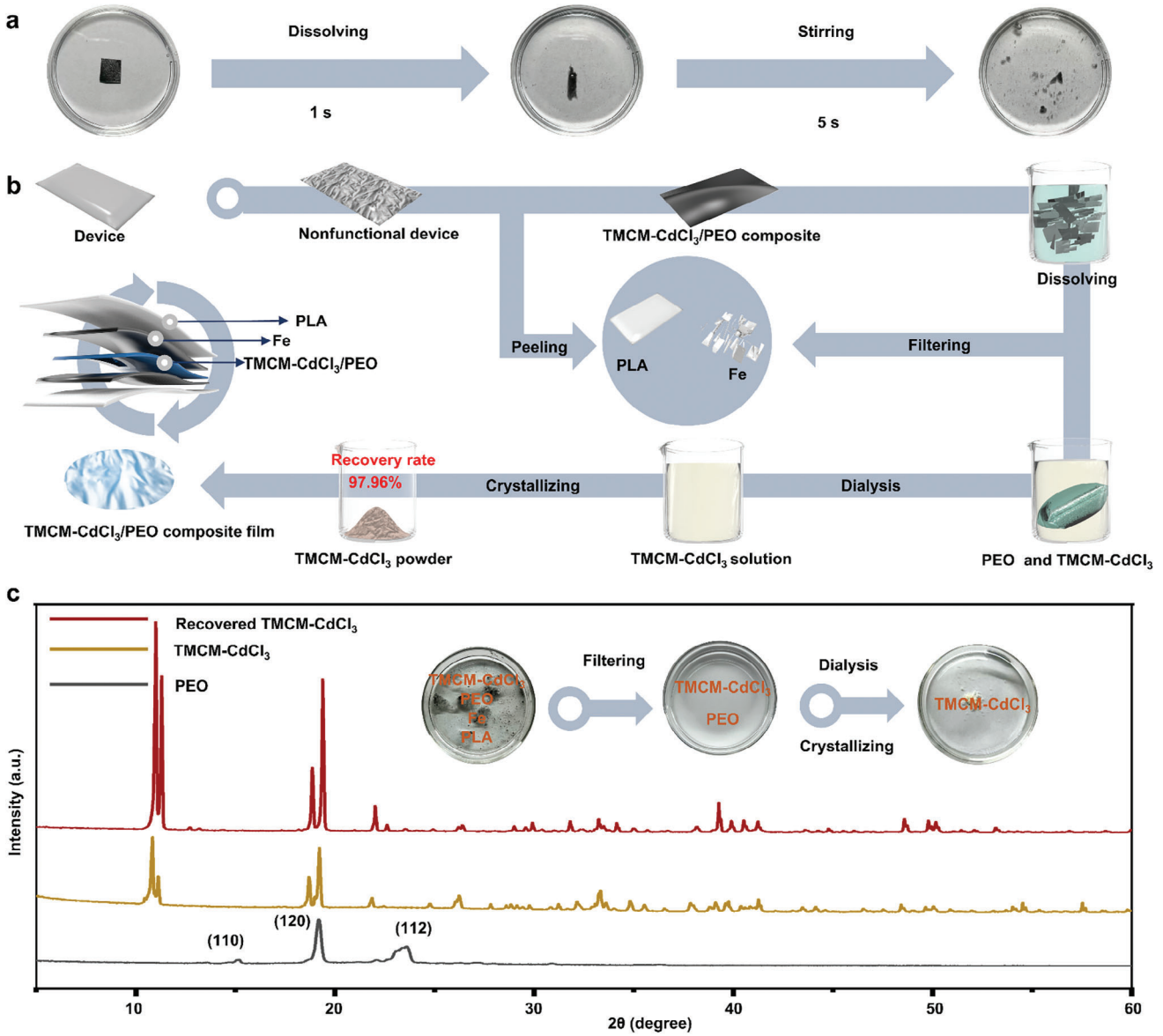

Figure 6. Dissolution and recycling of piezoelectric film components. a) Dissolution of the TMCM-$CdCl_3$/PEO composite film in water in a few seconds. b) Schematic of the separation and recycling of sensor components. c) XRD pattern of the recovered TMCM-$CdCl_3$.

3. Conclusion

We prepared a two-component crystal-based flexible composite film (TMCM-$CdCl_3$/PEO) with optimal piezoelectric performance by co-dissolution–evaporation method. Water-soluble polymers with different functional groups tended to form bonding interactions with the two components of TMCM-$CdCl_3$ in solution, exhibiting varying inhibitory effects on the crystallization of TMCM-$CdCl_3$ in the composite films and diminishing the piezoelectric performance of the films. The TMCM-$CdCl_3$/PEO film exhibited the highest d_{33} value because PEO lacks electrophilic or nucleophilic side-chain groups and therefore exhibits relatively weaker and fewer bonding interactions with the crystal components. Furthermore, slightly increasing the amount of one crystal component (TMCM-Cl or $CdCl_2$) gave it an advantage in competing against PEO for bonding with the other crystal component, thereby improving the coordination and co-crystallization yield of the two crystal components and further enhancing d_{33} to ≈71 pC/N, which exceeded that of the commercial piezoelectric PVDF and most other molecular ferroelectric crystal-based flexible films. The related mechanisms can be applied to the preparation of multi-component piezoelectric crystals-based flexible films in general. Owing to its rapid dissolution in water, the TMCM-$CdCl_3$/PEO film has immense potential in flexible piezoelectric sensors that display water-triggered degradation. Thus, this study revealed two novel ways and theories about using bonding optimization strategies to prepare multi-component crystal-based flexible films with high piezoelectric performance.

4. Experimental Section

Materials: PEO (Mv ≈1 000 000), PVA (alcoholysis degree 97.5–99 mol%), gelatin (glue strength ≈250 g Bloom), PAM (Mv ≈2 000 000–14 000 000), pullulan, PAA (Mv ≈450 000), cadmium chloride ($CdCl_2$, 99.0%), hydrochloric acid (HCl, 37 wt.%), and trimethylamine ($N(CH_3)_3$, 30 wt.% solution in water) were purchased from Aladdin. PLA was purchased from Lake Shore Biomaterials. PCL (Mv ≈80 000) and dichloromethane (CH_2Cl_2, AR, 99.5%) were purchased from Innochem. Polyurethane (PU), acetonitrile (CH_3CN, AR, 99.0%), DMF (AR, 99%), iron chloride hexahydrate ($FeCl_3{\cdot}6H_2O$, AR, 99%), and tetramethylammonium chloride ($(CH_3)_4NCl$, AR) were purchased from Macklin.

Preparation of TMCM-Cl and TMCM-$CdCl_3$: Equimolar amounts of $N(CH_3)_3$ in solution and CH_2Cl_2 were mixed in CH_3CN and reacted at ambient temperature for 48 h. The reaction mixture was then subjected to vacuum rotary evaporation to obtain trimethylchloromethyl ammonium chloride (TMCM-Cl) as a white solid. Single crystals of TMCM-$CdCl_3$ were prepared by co-dissolving TMCM-Cl and $CdCl_2$ in water at a 1:1 molar ratio, followed by evaporation, until forming TMCM-$CdCl_3$ single crystals.[15]

Preparation of Piezoelectric Crystal/Polymer Composite Films: TMCM-Cl and $CdCl_2$ were dissolved in a 1:1 molar ratio in deionized water to obtain an aqueous solution containing the crystal precursors. (This aqueous solution can also be obtained by directly dissolving TMCM-$CdCl_3$ crystals in deionized water.) Separately, a certain amount of PEO or another water-soluble polymer was dissolved in deionized water. These two aqueous solutions were then evenly mixed and poured into polytetrafluoroethylene (PTFE) Petri dishes (diameter of 66 mm) (Figure S24, Supporting Information). After drying the mixed solution in an air oven at 40 °C for 48 h, the TMCM-$CdCl_3$/PEO composite films were obtained.

TMCM-$CdCl_3$/PEO composite films were prepared with different mass ratios of TMCM-$CdCl_3$:PEO from 1:3 to 2:1 by varying the amounts of TMCM-$CdCl_3$ in the solution.

While fixing the mass ratio of TMCM-$CdCl_3$:PEO at 3:2, TMCM-$CdCl_3$/PEO films were prepared with an excess of one crystal component by increasing the amount of either TMCM-Cl or $CdCl_2$ in the solution. The mass ratios of TMCM-Cl to $CdCl_2$ ranged from 2:1 to 1:2.

The $[(CH_3)_4N][FeCl_4]$/polymer composite films were prepared similarly as described above. The difference was that a small amount of hydrochloric acid was added to avoid hydrolysis.[47]

Fabrication of Piezoelectric Sensors: Iron was deposited on both sides of the prepared TMCM-$CdCl_3$/PEO piezoelectric films by magnetron sputtering (Discovery 635, Denton Vacuum, USA). The sputtered films were cut into rectangular pieces measuring 1 cm × 1.5 cm. Two copper wires were connected to the iron electrode. The piezoelectric films with deposited iron were packaged using heat-sealing technology with PLA films.[71]

Dissolution and Recycling of Sensor Components: The TMCM-$CdCl_3$/PEO piezoelectric film in the sensor was mechanically separated from the PLA encapsulation layers. The separated film was soaked in water for a few minutes until it completely dissolved, and trace amounts of insoluble Fe were removed from the solution. Thereafter, the solution was poured into a dialysis bag (cellulose membrane with a weight cut-off of 500 D), which was placed in a beaker containing hundreds of milliliters of deionized water, and stirred gently for several hours. The dialysis process was repeated by replacing the deionized water in the beaker. The TMCM-$CdCl_3$ crystals were recrystallized from the dialysate by evaporating the water. PEO was precipitated and recycled from the solution in the dialysis bag by evaporation.

Characterization and Measurement: The morphology and elemental composition of the TMCM-$CdCl_3$/PEO piezoelectric films were examined using SEM (SU8020, HITACHI, Japan) and EDS, respectively.[72,73] The crystalline structures were analyzed via XRD (X'Pert Powder, Netherlands) with Cu Kα radiation. The piezoelectric coefficient d_{33} was determined using a quasi-static d_{33} piezometer (ZJ-4AN, IACAS, China). The mechanical properties of the films were characterized using DMA (Q800, TA, USA). A linear motor (LinMot, E1100) was used to apply a periodic force to devices based on the TMCM-$CdCl_3$/PEO piezoelectric films, and the electrical output data were collected using a digital oscilloscope (HDO6104, Teledyne LeCroy) and an electrometer (6517B, Keithley).

The human participants in the experiments received the informed signed consent. The wearable experiments were approved by the Committee on Ethics of the Beijing Institute of Nanoenergy and Nanosystems (Approval No. 2024016LZ).

Supporting Information

Supporting Information is available from the Wiley Online Library or from the author.

Acknowledgements

This work was supported by the National Key Research and Development Program of China (2022YFB3804700), the Natural Science Foundation of Beijing Municipality (L245015, Z240022), National Natural Science Foundation of China (T2125003, 52203325), and the Fundamental Research Funds for the Central Universities.

Conflict of Interest

The authors declare no conflict of interest.

Data Availability Statement

The data that support the findings of this study are available from the corresponding author upon reasonable request.

Keywords

bonding optimization, flexible film, multi-component crystal, piezoelectricity, soluble polymer

Received: August 6, 2024
Revised: October 31, 2024
Published online:

[1] G. Lee, Y. S. Choi, H.-J. Yoon, J. A. Rogers, *Matter* **2020**, *3*, 1031.
[2] J. T. Reeder, Z. Xie, Q. Yang, M. H. Seo, Y. Yan, Y. Deng, K. R. Jinkins, S. R. Krishnan, C. Liu, S. McKay, E. Patnaude, A. Johnson, Z. Zhao, M. J. Kim, Y. Xu, I. Huang, R. Avila, C. Felicelli, E. Ray, X. Guo, W. Z. Ray, Y. Huang, M. R. MacEwan, J. A. Rogers, *Science* **2022**, *377*, 109.
[3] Y. Wang, Z. Ma, P. Liu, W. He, *Chem. Eng. J.* **2023**, *473*, 144981.
[4] N. Mittal, A. Ojanguren, M. Niederberger, E. Lizundia, *Adv. Sci.* **2021**, *8*, 2004814.
[5] Y. Liu, G. Dzidotor, T. T. Le, T. Vinikoor, K. Morgan, E. J. Curry, R. Das, A. McClinton, E. Eisenberg, L. N. Apuzzo, K. T. M. Tran, P. Prasad, T. J. Flanagan, S.-W. Lee, H.-M. Kan, M. T. Chorsi, K. W. H. Lo, C. T. Laurencin, T. D. Nguyen, *Sci. Transl. Med.* **2022**, *14*, abi7282.
[6] T. Liu, Y. Wang, M. Hong, J. Venezuela, W. Shi, M. Dargusch, *Nano Today* **2023**, *52*, 101945.
[7] Y. Bai, H. Meng, Z. Li, Z. L. Wang, *Med. Mat.* **2024**, *1*, 40.
[8] X. Gao, J. Wu, Y. Yu, Z. Chu, H. Shi, S. Dong, *Adv. Funct. Mater.* **2018**, *28*, 1706895.
[9] M. T. Chorsi, E. J. Curry, H. T. Chorsi, R. Das, J. Baroody, P. K. Purohit, H. Ilies, T. D. Nguyen, *Adv. Mater.* **2019**, *31*, 1802084.
[10] D. Kim, S. A. Han, J. H. Kim, J.-H. Lee, S.-W. Kim, S.-W. Lee, *Adv. Mater.* **2020**, *32*, 1906989.

[11] R. Wang, J. Sui, X. Wang, *ACS Nano* **2022**, *16*, 17708.
[12] W.-Q. Liao, D. Zhao, Y.-Y. Tang, Y. Zhang, P.-F. Li, P.-P. Shi, X.-G. Chen, Y.-M. You, R.-G. Xiong, *Science* **2019**, *363*, 1206.
[13] X. G. Chen, Y. Y. Tang, H. P. Lv, X. J. Song, H. Peng, H. Yu, W. Q. Liao, Y. M. You, R. G. Xiong, *J. Am. Chem. Soc.* **1936**, *145*, 1936.
[14] T. Zhang, K. Xu, J. Li, L. He, D.-W. Fu, Q. Ye, R.-G. Xiong, *Natl. Sci. Rev.* **2023**, *10*, nwac240.
[15] Y.-M. You, W.-Q. Liao, D. Zhao, H.-Y. Ye, Y. Zhang, Q. Zhou, X. Niu, J. Wang, P.-F. Li, D.-W. Fu, Z. Wang, S. Gao, K. Yang, J.-M. Liu, J. Li, Y. Yan, R.-G. Xiong, *Science* **2017**, *357*, 306.
[16] Z.-X. Gu, N. Zhang, Y. Zhang, B. Liu, H.-H. Jiang, H.-M. Xu, P. Wang, Q. Jiang, R.-G. Xiong, H.-Y. Zhang, *Nat. Commun.* **2024**, *15*, 4416.
[17] Y. Ai, Z.-X. Gu, P. Wang, Y.-Y. Tang, X.-G. Chen, H.-P. Lv, P.-F. Li, Q. Jiang, R.-G. Xiong, J.-J. Zhang, H.-Y. Zhang, *Adv. Mater.* **2024**, *36*, 2405981.
[18] Z.-X. Zhang, X.-J. Song, Y.-R. Li, X.-G. Chen, Y. Zhang, H.-P. Lv, Y.-Y. Tang, R.-G. Xiong, H.-Y. Zhang, *Angew. Chem., Int. Ed.* **2022**, *61*, 202210809.
[19] Y.-J. Gong, Z.-G. Li, H. Chen, T.-M. Guo, F.-F. Gao, G.-J. Chen, Y. Zhang, Y.-M. You, W. Li, M. He, X.-H. Bu, J. Yu, *Matter* **2023**, *6*, 2066.
[20] F. Yang, J. Li, Y. Long, Z. Zhang, L. Wang, J. Sui, Y. Dong, Y. Wang, R. Taylor, D. Ni, W. Cai, P. Wang, T. Hacker, X. Wang, *Science* **2021**, *373*, 337.
[21] E. S. Hosseini, L. Manjakkal, D. Shakthivel, R. Dahiya, *ACS Appl. Mater. Interfaces* **2020**, *12*, 9008.
[22] H.-Y. Zhang, Y.-Y. Tang, Z.-X. Gu, P. Wang, X.-G. Chen, H.-P. Lv, P.-F. Li, Q. Jiang, N. Gu, S. Ren, R.-G. Xiong, *Science* **2024**, *383*, 1492.
[23] H. Y. Liu, H. Y. Zhang, X. G. Chen, R. G. Xiong, *J. Am. Chem. Soc.* **2020**, *142*, 15205.
[24] H.-Y. Zhang, Y.-Y. Tang, P.-P. Shi, R.-G. Xiong, *Acc. Chem. Res.* **2019**, *52*, 1928.
[25] R. Xu, Y. Wu, Y. Ma, Y. Zhang, S. Ma, M. Cai, F. Zhou, W. Liu, *Chem. Eng. J.* **2021**, *425*, 127249.
[26] L. J. Karas, C. H. Wu, R. Das, J. I. Wu, *Wiley Comput. Mol. Sci.* **2020**, *10*, 1477.
[27] G. Cavallo, P. Metrangolo, R. Milani, T. Pilati, A. Priimagi, G. Resnati, G. Terraneo, *Chem. Rev.* **2016**, *116*, 2478.
[28] E. Khare, N. Holten-Andersen, M. J. Buehler, *Nat. Rev. Mater.* **2021**, *6*, 421.
[29] I. Alkorta, J. Elguero, A. Frontera, *Crystals* **2020**, *10*, 180.
[30] Q. Yu, Y. Bai, Z. Li, F. Jiang, R. Luo, Y. Gai, Z. Liu, L. Zhou, Y. Wang, C. Li, K. Ren, D. Luo, H. Meng, Z. Li, *Nano Energy* **2024**, *121*, 109196.
[31] H. Meng, Q. Yu, Z. Liu, Y. Gai, J. Xue, Y. Bai, X. Qu, P. Tan, D. Luo, W. Huang, K. Nie, W. Bai, Z. Hou, R. Tang, H. Xu, Y. Zhang, Q. Cai, X. Yang, Z. L. Wang, Z. Li, *Matter* **2023**, *6*, 4274.
[32] W. Q. Liao, Y. Y. Tang, P. F. Li, Y. M. You, R. G. Xiong, *J. Am. Chem. Soc.* **2018**, *140*, 3975.
[33] H. Y. Zhou, Y. Ou, S. S. Yan, J. Xie, P. Zhou, L. Wan, Z. A. Xu, F. X. Liu, W. L. Zhang, Y. C. Xia, K. Liu, *Angew. Chem. Int. Ed.* **2023**, *62*, 202306948.
[34] M. Jaipal Reddy, P. P. Chu, *J. Power Sources* **2002**, *109*, 340.
[35] N. M. Zain, A. K. Arof, *Mater. Sci. Eng. B* **1998**, *52*, 40.
[36] H. Pang, C. Ma, Y. Shen, Y. Sun, J. Li, S. Zhang, L. Cai, Z. Huang, *ACS Appl. Mater. Interfaces* **2021**, *13*, 38732.
[37] P. Auffinger, F. A. Hays, E. Westhof, P. S. Ho, *Proc. Natl. Acad. Sci. USA* **2004**, *101*, 16789.
[38] A. R. Voth, P. Khuu, K. Oishi, P. S. Ho, *Nat. Chem.* **2009**, *1*, 74.
[39] C. B. Aakeröy, S. Panikkattu, P. D. Chopade, J. Desper, *CrystEngComm* **2013**, *15*, 3125.
[40] Y.-S. Xue, F.-Y. Jin, L. Zhou, M. P. Liu, Y. Xu, H.-B. Du, M. Fang, X.-Z. You, *Cryst. Growth Des.* **2012**, *12*, 6158.
[41] F. F. Awwadi, D. Taher, S. F. Haddad, M. M. Turnbull, *Cryst. Growth Des.* **2014**, *14*, 1961.
[42] Y. V. Torubaev, I. V. Skabitsky, K. A. Lyssenko, *Mendeleev Commun.* **2020**, *30*, 580.
[43] C. Wang, D. Danovich, Y. Mo, S. Shaik, *J. Chem. Theory Comput.* **2014**, *10*, 3726.
[44] C. Dong, M. Lu, H. Fan, Z. Jin, *J. Mater. Chem. B* **2022**, *10*, 9258.
[45] D. A. Decato, A. M. S. Riel, J. H. May, V. S. Bryantsev, O. B. Berryman, *Angew. Chem. Int. Ed.* **2021**, *60*, 3685.
[46] C. C. Robertson, J. S. Wright, E. J. Carrington, R. N. Perutz, C. A. Hunter, L. Brammer, *Chem. Sci.* **2017**, *8*, 5392.
[47] J. Harada, N. Yoneyama, S. Yokokura, Y. Takahashi, A. Miura, N. Kitamura, T. Inabe, *J. Am. Chem. Soc.* **2018**, *140*, 346.
[48] Z. Wang, Q. Lu, C. Liu, H. Tian, J. Wang, L. Xie, Q. Liu, H. Zeng, *Environ. Sci. Technol.* **2024**, *58*, 3412.
[49] Q. Lu, Z. Wang, J. Wang, L. Xie, Q. Liu, H. Zeng, *Chem. Eng. J.* **2023**, *470*, 144097.
[50] G. Kresse, J. Furthmüller, *Phys. Rev. B* **1996**, *54*, 11169.
[51] J. P. Perdew, K. Burke, M. Ernzerhof, *Phys. Rev. Lett.* **1996**, *77*, 3865.
[52] S. Grimme, J. Antony, S. Ehrlich, H. Krieg, *J. Chem. Phys.* **2010**, *132*, 154104.
[53] R. Dronskowski, P. E. Bloechl, *J. Phys. Chem.* **1993**, *97*, 8617.
[54] H. P. Lv, W. Q. Liao, Y. M. You, R. G. Xiong, *J. Am. Chem. Soc.* **2022**, *144*, 22325.
[55] R. Pandey, G. Sb, S. Grover, S. K. Singh, A. Kadam, S. Ogale, U. V. Waghmare, V. R. Rao, D. Kabra, *ACS Energy Lett.* **2019**, *4*, 1004.
[56] S. Mondal, T. Paul, S. Maiti, B. K. Das, K. K. Chattopadhyay, *Nano Energy* **2020**, *74*, 104870.
[57] A. A. Khan, G. Huang, M. M. Rana, N. Mei, M. Biondi, S. Rassel, N. Tanguy, B. Sun, Z. Leonenko, N. Yan, C. Wang, S. Xu, D. Ban, *Nano Energy* **2021**, *86*, 106039.
[58] T. Paul, S. Maiti, U. Mukherjee, S. Mondal, A. Sahoo, K. K. Chattopadhyay, *Mater. Lett.* **2021**, *301*, 130264.
[59] Z. Mallick, V. Gupta, A. Jain, C. Bera, D. Mandal, *Langmuir* **2023**, *39*, 320.
[60] W. Zhu, A. A. Khan, M. M. Rana, R. Gautheron-Bernard, N. R. Tanguy, N. Yan, P. Turban, S. Ababou-Girard, D. Ban, *ACS Omega* **2022**, *7*, 10559.
[61] R. Ding, X. Zhang, G. Chen, H. Wang, R. Kishor, J. Xiao, F. Gao, K. Zeng, X. Chen, X. W. Sun, Y. Zheng, *Nano Energy* **2017**, *37*, 126.
[62] A. A. Khan, M. M. Rana, G. Huang, N. Mei, R. Saritas, B. Wen, S. Zhang, P. Voss, E.-A. Rahman, Z. Leonenko, S. Islam, D. Ban, *J. Mater. Chem. A* **2020**, *8*, 13619.
[63] S. Ippili, V. Jella, J.-H. Eom, J. Kim, S. Hong, J.-S. Choi, V.-D. Tran, N. Van Hieu, Y.-J. Kim, H.-J. Kim, S.-G. Yoon, *Nano Energy* **2019**, *57*, 911.
[64] Z. Mallick, D. Saini, R. Sarkar, T. K. Kundu, D. Mandal, *Nano Energy* **2022**, *100*, 107451.
[65] A. Sultana, S. K. Ghosh, M. M. Alam, P. Sadhukhan, K. Roy, M. Xie, C. R. Bowen, S. Sarkar, S. Das, T. R. Middya, D. Mandal, *ACS Appl. Mater. Interfaces* **2019**, *11*, 27279.
[66] J. Nie, L. Zhu, W. Zhai, A. Berbille, L. Li, Z. L. Wang, *ACS Appl. Electron. Mater.* **2021**, *3*, 2136.
[67] M. T. Chorsi, T. T. Le, F. Lin, T. Vinikoor, R. Das, J. F. Stevens, C. Mundrane, J. Park, K. T. M. Tran, Y. Liu, J. Pfund, R. Thompson, W. He, M. Jain, M. D. Morales-Acosta, O. R. Bilal, K. Kazerounian, H. Ilies, T. D. Nguyen, *Sci. Adv.* **2023**, *9*, adg6075.
[68] H. Xue, J. Jin, Z. Tan, K. Chen, G. Lu, Y. Zeng, X. Hu, X. Peng, L. Jiang, J. Wu, *Sci. Adv.* **2024**, *10*, adn0260.
[69] X. Wan, Z. Wang, X. Zhao, Q. Hu, Z. Li, Z. L. Wang, L. Li, *Chem. Eng. J.* **2023**, *451*, 139077.
[70] P. Tan, X. Han, Y. Zou, X. Qu, J. Xue, T. Li, Y. Wang, R. Luo, X. Cui, Y. Xi, L. Wu, B. Xue, D. Luo, Y. Fan, X. Chen, Z. Li, Z. L. Wang, *Adv. Mater.* **2022**, *34*, 2200793.
[71] Q. Zheng, Y. Zou, Y. Zhang, Z. Liu, B. Shi, X. Wang, Y. Jin, H. Ouyang, Z. Li, Z. L. Wang, *Sci. Adv.* **2016**, *2*, 1501478.
[72] K. Baker, I. Zhitomirsky, *Micro* **2022**, *2*, 154.
[73] J. Thomason, *Micro* **2023**, *3*, 353.